Journal of Statistical Physics, Vol. 127, No. 2, April 2007 (© 2007)
DOI: 10.1007/s10955-006-9236-2

Dynamic Dipole and Quadrupole Phase Transitions in the Kinetic Spin-3/2 Model

Mustafa Keskin,[1] Osman Canko[1] and Muharrem Kırak[2]

Received July 13, 2006; accepted October 9, 2006
Published Online: February 23, 2007

The dynamic phase transition has been studied, within a mean-field approach, in the kinetic spin-3/2 Ising model Hamiltonian with arbitrary bilinear and biquadratic pair interactions in the presence of a time dependent oscillating magnetic field by using the Glauber-type stochastic dynamics. The nature (first- or second-order) of the transition is characterized by investigating the behavior of the thermal variation of the dynamic order parameters and as well as by using the Liapunov exponents. The dynamic phase transitions (DPTs) are obtained and the phase diagrams are constructed in the temperature and magnetic field amplitude plane and found nine fundamental types of phase diagrams. Phase diagrams exhibit one, two or three dynamic tricritical points, and besides a disordered (D) and the ferromagnetic-3/2 ($F_{3/2}$) phases, six coexistence phase regions, namely $F_{3/2} + F_{1/2}$, $F_{3/2} + D$, $F_{3/2} + F_{1/2} + FQ$, $F_{3/2} + FQ$, $F_{3/2} + FQ + D$ and $FQ + D$, exist in which depending on the biquadratic interaction.

KEY WORDS: spin-3/2 Ising model, Glauber-type stochastic dynamics, dynamic phase transitions, phase diagram.

PACS number(s): 05.50.+q, 05.70.Fh, 64.60.Ht, 75.10.Hk

1. INTRODUCTION

The spin-3/2 Ising model, Hamiltonian with arbitrary bilinear (J) and biquadratic (K) nearest-neighbor interactions, has been introduced earlier[1] to give a qualitative description of phase transitions observed in the compound $DyVO_4$ within the mean-field approximation (MFA). Subsequently, the equilibrium properties of the model have been studied by well known methods in equilibrium statistical physics such as the mean-field approximation, the cluster variation method, the effective field theory, the renormalization-group techniques and Monte Carlo simulations.

[1] Department of Physics, Erciyes University, 38039 Kayseri, Turkey.
[2] Institute of Science, Erciyes University, 38039 Kayseri, Turkey.

While the equilibrium properties of the model have extensively been investigated by many different methods, the nonequilibrium properties of the model have not been as thoroughly explored. An early attempt to study the dynamics of the model was done by means of the Onsager's theory of irreversible thermodynamics or the Onsager reciprocity theorem (ORT), in particular, three relaxation times were calculated and examined for the temperatures near the second-order phase transition temperatures.[2] Recently, the nonequilibrium properties of the model were studied by using the path probability method (PMM) with point distribution, especially the relaxation of order parameters was investigated and the nonequilibrium behavior of the model was also shown in a three dimensional phase space.[3] We should also mention that a spin-3/2 Ising system containing the crystal-field interaction (D) in addition to J interaction is often called the spin-3/2 Blume-Capel (BC) model, and the spin-3/2 Ising model Hamiltonian with J, K and D interactions is known as the spin-3/2 Blume-Emery-Griffiths (BEG) model. The dynamical aspects of the spin-3/2 BC model have been studied by Grandi and Figueiredo[4] using Monte Carlo simulations and by Keskin *et al*.[5] using the Glauber-type stochastic dynamics.[6] Moreover, the DPTs in the kinetic spin-3/2 BEG model have been studied within the Glauber-type stochastic dynamics by Canko *et al*.[7]

The purpose of the present paper is, therefore, to study within mean-field approach the stationary states of the spin-3/2 Ising model Hamiltonian with only J and K interaction in the presence of a time dependent oscillating external magnetic field. We employ the Glauber transition rates to construct the mean-field dynamical equations and solve these equations.[6] Especially, we investigate the time dependence of average magnetization and the quadrupole moment, and the behavior of the dynamic order parameters as a function of the temperature. In these studies, we obtain the (DPT) points and construct the phase diagrams in the temperature and magnetic field amplitude plane. We also calculate the Liapunov exponents to verify the stability of solutions and the DPT points. Thus, we will find the influence of the biquadratic exchange interaction (K). The influence of K is very important, because it produces the ferroquadrupolar or simply the quadrupolar phase; hence one has to consider the quadrupolar order parameters besides the magnetization. Moreover, the equations of motion become the coupled differential equations. This type of calculation was first applied to a kinetic spin-1/2 Ising system by Tomé and Oliveira[8] and then used to study kinetics of a classical mixed spin-1/2 and spin-1 Ising system by Buendia and Machado,[9] kinetics of spin-1 Ising systems,[10,11] spin-3/2 BC model by Keskin *et al*.[5] and kinetic spin-3/2 BEG model by Canko *et al*.[7]

It is worthwhile to mention that the existence of quadrupolar interactions has been established in several cubic rare-earth intermetallic compounds.[12] The most obvious proof is the possibility of a quadrupolar phase transition, as observed, for example, in TmCd[13] and TmZn.[14] Moreover, the quadrupolar interactions may act on the nature of the magnetic phase transition in which they may change a

second-order phase transition into a first-order one, as observed, e.g., DySb,[15] TbP[16] or TmCu,[17] or vice versa as in $PrMg_2$.[18] On the other hand, numerous theoretical works have been worked out concerning the existence of dipolar and quadrupolar phase transitions, especially in the Ising systems, such as spin-1,[19–21] spin-3/2[1,22] and spin-2.[23] Magnetic dipolar and quadrupolar phase transitions in cubic rare-earth intermetallic compounds have been studied in terms of single-ion susceptibilities and within the Landau theory.[24] Recently, the quadrupolar order in the $S = 1$ isotropic Heissenberg model with the biquadratic interaction has been studied by the quantum Monte Carlo simulation.[25]

We should also mention that the (DPT) is one of the characteristic behaviors in nonequilibrium system at the presence of an oscillating external magnetic field and has attracted much attention recent years. The DPT was first found in a study within a mean-field approach of the stationary states of the kinetic spin-1/2 Ising model under a time-dependent oscillating field,[8,26] by using Glauber-type stochastic dynamics,[7] and it was followed by Monte Carlo simulation, which allows the microscopic fluctuation, and research of kinetic spin-1/2 Ising models,[27–30] as well as further mean-field studies.[31] Moreover, Tutu and Fujiwara[32] developed the systematic method to get the phase diagrams in DPTs, and constructed the general theory of DPTs near the transition point based on mean-field description, such as Landau's general treatment of the equilibrium phase transitions. The DPT has also been found in a one-dimensional kinetic spin-1/2 Ising model with boundaries.[33] Experimental evidences for the DPT have been found in highly anisotropic (Ising-like) and ultrathin Co/Cu (001) ferromagnetic films[34] and in ferroic system (ferromagnets, ferroelectrics and ferroelastics) with pinned domain walls.[35] Furthermore, we should also mention that recent researches on the DPT are widely extended to more complex systems such as vector type order parameter system, e.g., the Heisenberg-spin systems,[36] XY model,[37] a Ziff-Gulari-Barshad model for CO oxidation with CO desorption to periodic variation of the CO pressure[38] and high-spin Ising models such as kinetics of spin-1 Ising systems,[10,11] spin-3/2 BC model[5] and spin-3/2 BEG model,[7] and kinetics of a mixed spin Ising ferromagnetic system.[9] The DTP in model ferromagnetic systems (Ising and Heisenberg) in the presence of sinusoidally oscillating magnetic field have been reviewed by Acharyya, recently.[39]

The outline of the remaining part of this paper is organized as follows. In Sec. 2, the model is presented briefly and the derivation of the mean-field (MF) dynamic equations of motion is given by using the Glauber-type stochastic dynamics in the presence of a time-dependent oscillating external magnetic field. In Sec. 3, stationary solutions of the coupled dynamic equations are solved and the thermal behaviors of the dynamic order parameters are studied, and as a result, the DPT points are calculated. Moreover, we also calculate the Liapunov exponents to verify the stability of a solution and the DPT points. Section 4 contains the

presentation and discussion of the phase diagrams. Finally, a summary is given in Sec. 5.

2. THE MODEL AND DERIVATION OF MEAN-FIELD DYNAMIC EQUATIONS OF MOTION

Since the model is a specific version of the system in Ref. 7 and the method is the same in Ref. 7, hence we shall give a summary in here. The Hamiltonian of spin-3/2 Ising model with arbitrary bilinear and biquadratic pair interactions is given by

$$H = -J \sum_{\langle ij \rangle} S_i S_j - K \sum_{\langle ij \rangle} \left[S_i^2 - 5/4\right]\left[S_j^2 - 5/4\right] - H \sum_i S_i, \qquad (1)$$

where the spin located at site i on a discrete lattice can take values $\pm 3/2$ and $\pm 1/2$ at each site i of a lattice and $\langle ij \rangle$ indicates a summation over all pairs of nearest-neighboring sites. J and K are, respectively, the nearest-neighbor bilinear and biquadratic exchange constants, and H is a time-dependent oscillating external magnetic field. H is given by $H(t) = H_0 \cos(\omega t)$, where H_0 and $\omega = 2\pi\nu$ are the amplitude and the angular frequency of the oscillating field, respectively. The system is in contact with an isothermal heat bath at absolute temperature.

The order parameters of the system are introduced as follows: (1) The average magnetization $m = \langle S_i \rangle$, which is the excess of one orientation over the other orientation, also called the dipole moment. (2) The quadrupole moment q, which is a linear function of the average squared magnetization, i.e. $q = \langle S_i^2 \rangle - 5/4$, which is different from the definition $q = \langle S_i^2 \rangle$ used by some researchers.[40] The first definition ensures that $q = 0$ at infinite temperature. (3) The octupolar moment r, which is the odd functions of average magnetization $\langle S_i \rangle$ and defined as $r = 5/3\langle S_i^3 \rangle - 41/12\langle S_i \rangle$. This definition also ensures that $r = 0$ at infinite temperature, and this is different from the definition $r = \langle S_i^3 \rangle$ used by some researchers.[41] We should also mention that since the behavior of r is similar to the behavior of s, we will not use r as many researchers have done.

Now, we will employ the Glauber transition rates to construct the dynamic equations of motion. Hence, the system evolves according to a Glauber-type stochastic process at a rate of $1/\tau$ transitions per unit time. We define $\mathbf{P} = P(S_1, S_2, \ldots S_i \ldots, S_N; t)$ as the probability that the system has the S-spin configuration, $S_1, S_2, \ldots, S_N$, at time t. The time-dependence of this probability function is assumed to be governed by the master equation which describes the interaction between spins and heat bath and can be written as

$$\frac{d}{dt}\mathbf{P} = -\sum_i \left(\sum_{S_i \neq S_i'} W_i(S_i \to S_i') \right) \mathbf{P} + \sum_i \left(\sum_{S_i \neq S_i'} W_i(S_i' \to S_i) \mathbf{P}' \right), \qquad (2)$$

where $\mathbf{P}' = P(S_1, S_2, \ldots S_i' \ldots, S_N; t)$, $W_i(S_i \to S_i')$, the probability per unit time that the ith spin changes from the value S_i to S_i', and in this sense the Glauber model is stochastic. Since the system is in contact with a heat bath at absolute temperature T, each spin can change from the value S_i to S_i' with the probability per unit time;

$$W_i(S_i \to S_i') = \frac{1}{\tau} \frac{\exp(-\beta \Delta E(S_i \to S_i'))}{\sum_{S_i'} \exp(-\beta \Delta E(S_i \to S_i'))}, \tag{3}$$

where $\beta = 1/k_B T$, k_B is the Boltzmann factor, $\sum_{S_i'}$ is the sum over the four possible values of S_i', $\pm 3/2$, $\pm 1/2$ and

$$\Delta E(S_i \to S_i') = -\left(S_i' - S_i\right)\left(H + J \sum_{\langle j \rangle} S_j\right) - \left(S_i'^2 - S_i^2\right) K \sum_{\langle j \rangle} \left(S_j^2 - 5/4\right), \tag{4}$$

gives the change in the energy of the system when the S_i-spin changes. The probabilities satisfy the detailed balance condition. Since $W_i(S_i \to S_i')$ does not depend on the value S_i, we can write $W_i(S_i \to S_i') = W_i(S_i')$, then the master equation becomes

$$\frac{d}{dt}\mathbf{P} = -\sum_i \left(\sum_{S_i' \neq S_i} W_i(S_i')\right)\mathbf{P} + \sum_i W_i(S_i)\left(\sum_{S_i' \neq S_i} \mathbf{P}\right). \tag{5}$$

Since the sum of probabilities is normalized to one, by multiplying both sides of Eq. (5) by first S_k for m and $(S_k^2 - 5/4)$ for q then taking the averages; and finally by using a mean-field approach we obtain the set of the mean-field dynamical equations for the order parameters.

$$\Omega \frac{dm}{d\xi} = -m + \frac{3\exp(kq/T)\sinh[3(m + h\cos\xi)/2T] + \exp(-kq/T)\sinh[(m + h\cos\xi)/2T]}{2\exp(kq/T)\cosh[3(m + h\cos\xi)/2T] + 2\exp(-kq/T)\cosh[(m + h\cos\xi)/2T]}, \tag{6}$$

$$\tau \frac{dq}{dt} = -q + \frac{\exp(kq/T)\cosh[3(m + h\cos\xi)/2T] - \exp(-kq/T)\cosh[(m + h\cos\xi)/2T]}{\exp(kq/T)\cosh[3(m + h\cos\xi)/2T] + \exp(-kq/T)\cosh[(m + h\cos\xi)/2T]}, \tag{7}$$

where $m \equiv \langle S \rangle$, $q \equiv \langle S^2 \rangle - 5/4$, $\xi = \omega t$, $T = (\beta z J)^{-1}, k = K/J$, $h = H_0/zJ$, $\Omega = \tau\omega$. We fixed $z = 4$ and $\Omega = 2\pi$. The Solution and discussion of these equations are given in the next section.

3. THERMAL BEHAVIORS OF DYNAMIC ORDER PARAMETERS AND DYNAMIC PHASE TRANSITION POINTS

In this section, we shall first solve the set of dynamic equations and present the behaviors of average order parameters in a period as a function of reduced temperature, and as a result, the DPT points are calculated. Moreover, we also calculate the Liapunov exponents to verify the stability of solutions and the DPT points. For these purposes, first we have to study the stationary solutions of the set of dynamic equations, given in Eqs. (6) and (7), when the parameters k, h and T are varied. The stationary solutions of Eqs. (6) and (7) will be a periodic function of ξ with period 2π. Moreover, they can be one of three types according to whether they have or do not have the property

$$m(\xi + \pi) = -m(\xi) \quad \text{and} \quad q(\xi + \pi) = -q(\xi). \tag{8}$$

A solution satisfies Eq. (8) is called a symmetric solution which corresponds to a disordered (D) solution. In this solution, the magnetization $m(\xi)$ always oscillates around the zero value and is delayed with respect to the external magnetic field. On the other hand, the quadrupolar order parameters $q(\xi)$ oscillate around a nonzero value for finite temperatures and around the zero value for the infinite temperature due to the reason that $q = 0$ at the infinite temperature by the definition of q, given in Sec. 2. The second type of solution, which does not satisfy Eq. (8), is called a nonsymmetric solution that corresponds to a ferromagnetic solution. In this case, the magnetization and quadrupolar order parameters do not follow the external magnetic field any more, but instead of oscillating around the zero value; they oscillate around a nonzero value, namely $m(\xi)$ oscillates around either $\pm 3/2$ or $\pm 1/2$. Hence, if it oscillates around $\pm 3/2$, this nonsymmetric solution corresponds to the ferromagnetic $\pm 3/2$ ($F_{3/2}$) phase and if it oscillates around $\pm 1/2$, this corresponds to the ferromagnetic $\pm 1/2$ ($F_{1/2}$) phase. The third type of solution, which does satisfy the first term of Eq. (8) but does not satisfy the second term of Eq. (8), corresponds to ferroquadrupolar or simply quadrupolar (FQ) phase. In this solution, $m(\xi)$ oscillates around the zero value and is delayed with respect to the external magnetic field and $q(\xi)$ does not follow the external magnetic field any more, but instead of oscillating around the zero value, it oscillates around a nonzero value, namely either -1 or $+1$. Hence, if it oscillates around -1, this nonsymmetric solution corresponds to the ferroquadrupolar or simply quadrupolar (FQ) phase and if it oscillates around $+1$, this corresponds to the disordered phase (D). These facts are seen explicitly by solving Eqs. (6) and (7) numerically. Equations (6) and (7) are solved by using the numerical method of the Adams-Moulton predictor corrector method for a given set of parameters and initial values and presented in Fig. 1. From Fig. 1, one can see eight different solutions, i.e., the D, $F_{3/2}$ phases or solutions and six coexistence solutions, namely the $F_{3/2} + F_{1/2}$ in which $F_{3/2}$ and $F_{1/2}$ solutions coexist, the $F_{3/2} + D$ in

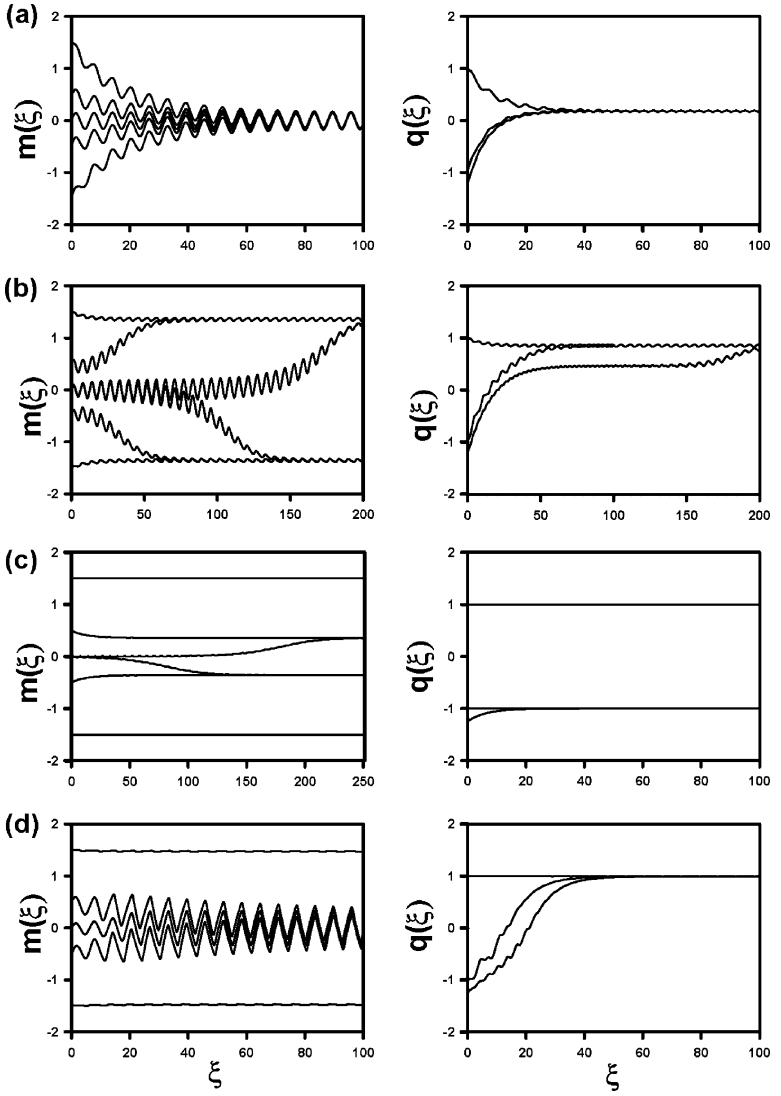

Fig. 1. Time variations of the magnetization (m) and the quadrupole moment (q): (a) Exhibiting a disordered phase (D), $k = 0.10$, $h = 1.25$ and $T = 1.375$. (b) Exhibiting a ferromagnetic phase ($F_{3/2}$), $k = 0.50$, $h = 0.75$ and $T = 0.25$. (c) Exhibiting a coexistence region ($F_{3/2} + F_{1/2}$), $k = 1.0$, $h = 0.075$ and $T = 0.125$. (d) Exhibiting a coexistence region ($F_{3/2} + D$), $k = 0.75$, $h = 1.125$ and $T = 0.375$. (e) Exhibiting a coexistence region ($F_{3/2} + F_{1/2} + FQ$), $k = 1.0$, $h = 0.35$ and $T = 0.05$. (f) Exhibiting a coexistence region ($F_{3/2} + FQ$), $k = 0.50$, $h = 0.50$ and $T = 0.125$.g Exhibiting a coexistence region ($F_{3/2} + FQ + D$), $k = 0.75$, $h = 1.125$ and $T = 0.125$. (h) Exhibiting a coexistence region ($FQ + D$), $k = 2.0$, $h = 1.75$ and $T = 0.75$.

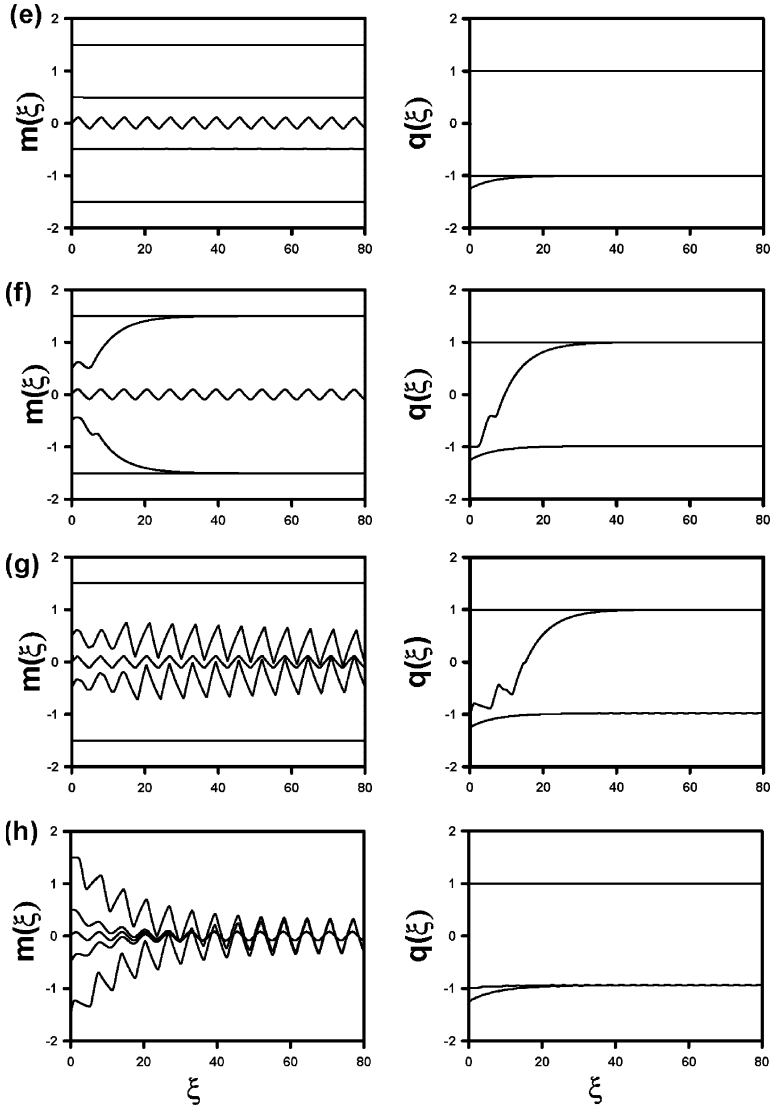

Fig. 1. Continued

which $F_{3/2}$ and D solutions coexist, the $F_{3/2} + F_{1/2} + FQ$ in which $F_{3/2}$, $F_{1/2}$ and FQ solutions coexist, the $F_{3/2} + FQ$ in which $F_{3/2}$ and FQ solutions coexist, the $F_{3/2} + FQ + D$ in which $F_{3/2}$, FQ, and D solutions coexist and the $FQ + D$ in which FQ and D solutions coexist, exist in the system. In Fig. 1(a) only the

symmetric solution is always obtained, hence, we have a disordered (D) solution, but in Fig. 1(b), only the nonsymmetric solution is found; therefore, we have a ferromagnetic ($F_{3/2}$) solution. These solutions do not depend on the initial values. In Fig. 1(c), we have the nonsysmmetric solution for $m(\xi)$ and $q(\xi)$, because $m(\xi)$ oscillates around either $\pm 3/2$ or $\pm 1/2$ values and $q(\xi)$ around ± 1, hence we have the coexistence solution ($F_{3/2} + F_{1/2}$). In Fig. 1(d), $m(\xi)$ oscillates around either $\pm 3/2$ or zero values and $q(\xi)$ around $+1$. As explained above, the solution of $q(\xi)$ which oscillates around $+1$ does not give a phase transition, see also Fig. 2(c) and it corresponds to the D phase, hence we have the coexistence solution ($F_{3/2} + D$). In Fig. 1(e), $m(\xi)$ oscillates around $\pm 3/2, \pm 1/2$ or zero values and $q(\xi)$ around ± 1, hence we have the coexistence solution ($F_{3/2} + F_{1/2} + FQ$). Moreover, in Fig. 1(f)–(h) we have the $F_{3/2} + FQ$, $F_{3/2} + FQ + D$ and $FQ + D$ coexistence solutions, respectively. We should also mention that the solutions shown in Fig. 1(c)–(h) depend on the initial values.

Thus, Fig. 1 displays that we have eight phases in the system, namely D, $F_{3/2}, F_{3/2} + F_{1/2}, F_{3/2} + D, F_{3/2} + F_{1/2} + FQ, F_{3/2} + FQ, F_{3/2} + FQ + D$ and $FQ + D$ solutions or phases. In order to see the dynamic boundaries among these eight phases, we have to calculate DPT points and then we can present phase diagrams of the system. DPT points will be obtained by investigating the behavior of the average order parameters in a period or the dynamic order parameters as a function of the reduced temperature. These investigations will also be checked and verified by calculating the Liapunov exponents.

The dynamic order parameters, namely the dynamic magnetization (M) and the dynamic quadruple moment (Q), are defined as

$$M = \frac{1}{2\pi} \int_0^{2\pi} m(\xi)\, d\xi \quad \text{and} \quad Q = \frac{1}{2\pi} \int_0^{2\pi} q(\xi) d\xi. \tag{9}$$

The behaviors of M and Q as a function of the reduced temperature for several values of h and k are obtained by combining the numerical methods of Adams-Moulton predictor corrector with the Romberg integration, and some results are plotted in Fig. 2(a)–(f) in order to illustrate the calculation of the DPT and the dynamic phase boundaries among eight phases, as a few examples. In the figures, thick and thin lines represent M and Q, respectively; T_C and T_t are the critical or the second-order phase transition and first-order phase transition temperatures for both M and Q, respectively and T_{tQ} is the first-order phase transition temperatures for only Q. Figure 2(a) represents the reduced temperature dependence of the dynamic order parameters, M and Q, for $k = 0.10$ and $h = 0.10$. In this case, M and Q decrease to zero continuously as the reduced temperature increases, therefore a second-order phase transition occurs and the phase transition is from the $F_{3/2}$ phase to the D phase. Figure 2(b) and (c) show the behavior of M and Q as a function of the reduced temperature for $k = 0.10$ and $h = 1.25$ for two different

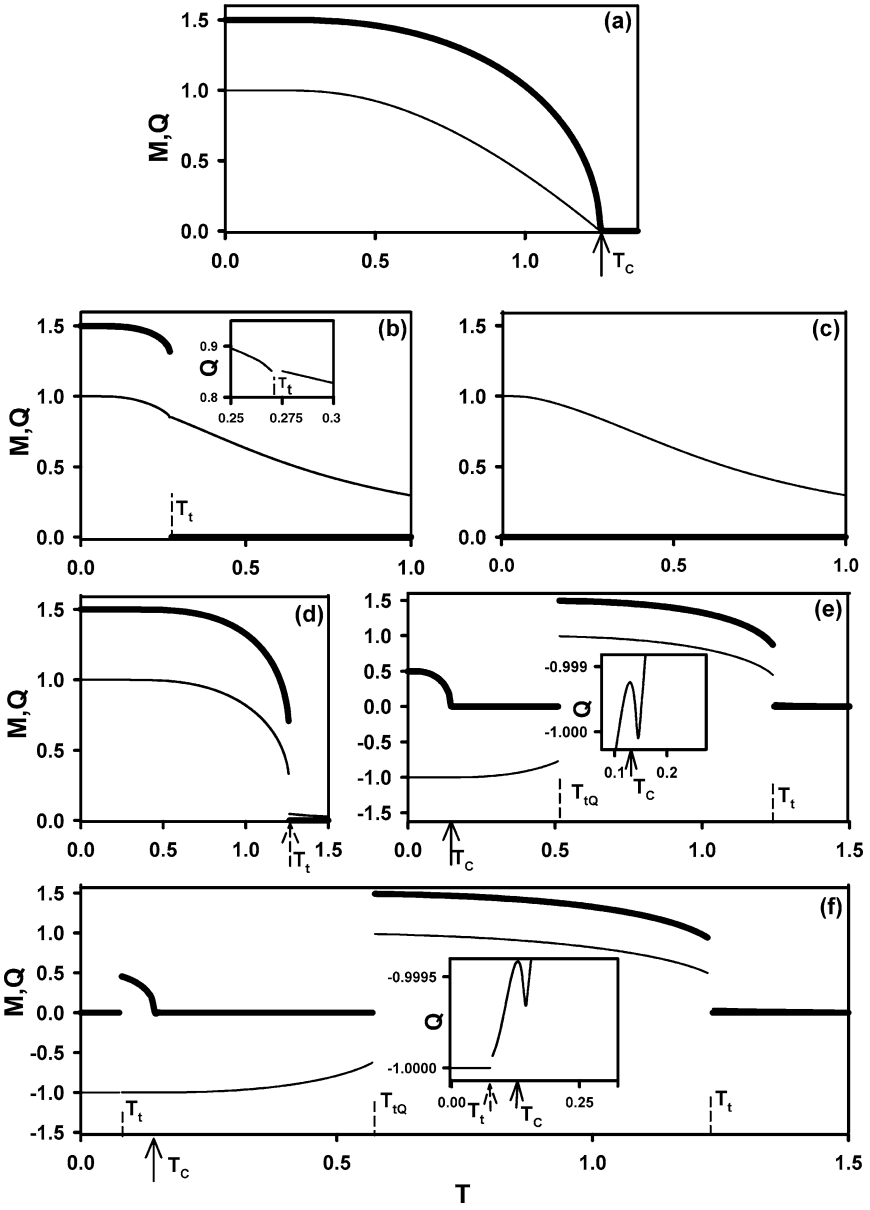
(a)
M,Q
1.5
1.0
0.5
0.0
0.0
0.5
1.0
T_C
(b)
Q
0.9
0.8
0.25
0.275
0.3
T_t
(c)
(d)
(e)
-0.999
-1.000
0.1
0.2
T_{tQ}
(f)
-0.9995
-1.0000
0.00
0.25
T

initial values; i.e., the initial value of M and Q are taken 3/2 and 1.0, respectively for Fig. 2(b) and $M = 0$ and $Q = 1.0$ for Fig. 2(c). In Fig. 2(b), both M and Q undergo a first-order phase transition, because M and Q decrease to zero discontinuously as the reduced temperature increases and the phase transition is from the $F_{3/2}$ phase to the D phase. Figure 2(c) shows that M always equals to zero and $Q = 1.0$ at zero temperature but does not undergo any phase transition and this implies that the nonsymmetric solution of $q(\xi)$ that oscillates around $+1$; hence this figure corresponds to the D phase. From Fig. 2(b) and (c), one can see that the system exhibits the $F_{3/2} + D$ coexistence phase region, compare Fig. 2(b) and (c), with Fig. 4(a). Figure 2(d)–(f) illustrate the thermal variations of M and Q for $k = 0.75$ and $h = 0.35$ for three different initial values; i.e., the initial values: $M = 3/2$, $Q = 1.0$ for Fig. 2(d), and $M = 1/2$and $Q = -1.0$ for Fig. 2(e), and $M = 0$ and $Q = -1.25$ for Fig. 2(f). The behavior of Fig. 2(d) is similar to Fig. 2(b), hence the system undergoes a first-order phase transition from the $F_{3/2}$ phase to the D phase. In Fig. 2(e), the system undergoes three successive phase transitions, the first one is a second-order from the $F_{1/2}$ phase to the FQ phase, the second one is a first-order from the FQ phase to the $F_{3/2}$ phase and the third one is also a first-order phase transition from the $F_{3/2}$ phase to the D phase. In Fig. 2(f), the system undergoes four successive phase transitions, the first one is a first-order from the FQ phase to the $F_{1/2}$ phase, the second one is a second-order from the $F_{1/2}$ phase to the FQ phase, the third one is a first-order phase transition from the FQ phase to the $F_{3/2}$ phase and the fourth one is also a first-order phase transition from the $F_{3/2}$ phase to the D phase. These three figures imply that the system exhibits the $F_{3/2} + F_{1/2} + FQ$ coexistence region or phase for very low values of temperature, then the $F_{3/2} + F_{1/2}$ phase, then the $F_{3/2} + FQ$ phase, then the $F_{3/2}$ phase, then the $F_{3/2} + D$

←

Fig. 2. The reduced temperature dependence of the dynamic magnetization (M) (the thick solid line) and the dynamic quadruple moment (Q) (the thin solid line). T_C and T_t are the critical or the second- and the first-order phase transition temperatures for both M and Q, respectively and T_{tQ} is the first-order phase transition temperature for only Q. (a) Exhibiting a second-order phase transition from the $F_{3/2}$ phase to the D phase for $k = 0.1$ and $h = 0.10$; 1.255 is found T_C. (b) Exhibiting a first-order phase transition from the $F_{3/2}$ phase to the D phase for $k = 0.1$ and $h = 1.25$; 0.275 is found T_t. (c) The system does not undergo any phase transition and corresponds to the D phase; $k = 0.1$ and $h = 1.25$. (d) Exhibiting a first-order phase transition from the $F_{3/2}$ phase to the D phase for $k = 0.75$ and $h = 0.35$; 1.265 is found T_t. (e) Exhibiting three successive phase transitions, the first one is a second-order from the $F_{1/2}$ phase to the FQ phase, the second one is a first-order from the FQ phase to the $F_{3/2}$ phase and the third one is also a first-order phase transition from the $F_{3/2}$ phase to the D phase for $k = 0.75$ and $h = 0.35$; 0.150, 0.515 and 1.245 found T_C, T_{tQ} and T_t, respectively. Q makes a peak at T_C, seen in the insert figure. (f) Exhibiting four successive phase transitions, the first one is a first-order from the FQ phase to the $F_{1/2}$ phase, the second one is a second-order from the $F_{1/2}$ phase to the FQ phase, the third one is a first-order phase transition from the FQ phase to the $F_{3/2}$ phase and the fourth one is also a first-order phase transition from the $F_{3/2}$ phase to the D phase for $k = 0.75$ and $h = 0.35$; 0.08, 0.150, 0.575 and 1.245 found T_t, T_C, T_{tQ} and T_t, respectively.

phase and finally D phase for very high values of the temperature. These facts are seen clearly in the phase diagram of Fig. 4(f) for $h = 0.35$ exists.

Now we can check and verify the stability of solutions, and as well as the DPT points by calculating the Liapunov exponents. If we write Eq. (9) as

$$\Omega \frac{dm}{d\xi} = F_1(m, \xi) \quad \text{and} \quad \Omega \frac{dq}{d\xi} = F_2(q, \xi), \tag{10}$$

then the Liapunov exponents λ_m and λ_q are given by

$$\Omega \lambda_m = \frac{1}{2\pi} \int_0^{2\pi} \frac{\partial F_1}{\partial m} d\xi \quad \text{and} \quad \Omega \lambda_q = \frac{1}{2\pi} \int_0^{2\pi} \frac{\partial F_2}{\partial q} d\xi. \tag{11}$$

When $\lambda_m < 0$ and $\lambda_q < 0$, the solutions are stable. We have two Liapunov exponents, namely, one is associated to the symmetric solution, λ_{ms} and λ_{qs}, and the other to the nonsymmetric solution, λ_{mn} and λ_{qn}, for both m and q. If λ_{mn} and λ_{ms} increase to zero continuously as the reduced temperature approaches the phase transition temperature, the temperature where $\lambda_{mn} = \lambda_{ms} = 0$ is the second-order phase transition temperature, T_C. Moreover, if the Liapunov exponents for q, e.g., $\lambda_{qn'}$ and $\lambda_{qn''}$ in Fig. 3(b), increase continuously as the reduced temperature approaches to the phase transition temperature and then the temperature where the Liapunov exponents make a cusp is the second-order phase transition temperature, T_C. The reason that Liapunov exponents for q are not zero at T_C due to the reason that Q is not zero at T_C and it is zero at infinite temperature, as mentioned in Sec. 2. On the other hand, if the Liapunov exponents approach the phase transition temperature, the temperature at which the Liapunov exponents make a jump discontinuity is the first-order phase transition temperature. In order to see these behaviors explicitly, the values of the Liapunov exponents are calculated and plotted as a function of reduced temperature for $k = 0.75$ and $h = 0.35$ (these values correspond to Fig. 2(e) because the initial value of M and Q are taken $+1/2$ and -1.0, respectively), seen in Fig. 3. In the figure, the thick and thin lines represent the λ_s and λ_n, respectively. In Fig. 3, the system undergoes three successive phase transitions: The first one is a second-order, because $\lambda_{mn'} = \lambda_{ms} = 0$ at $T_C = 0.150$ ($\lambda_{mn'}$ corresponds to the $F_{1/2}$ phase), seen in Fig. 3(a), the second one is a first-order, because of λ_{ms} and λ_{mn} make a jump discontinuity at $T_{tQ} = 0.515$ (λ_{mn} corresponds to the $F_{3/2}$ phase), and the third one is also a first-order phase transition, because of λ_{mn} and λ_{ms} make a jump discontinuity at $T_t = 1.245$. Figure 3(b) illustrates the behavior of Liapunov exponents for q. It is seen from this figure that, first $\lambda_{qn'}$ and $\lambda_{qn''}$ make a cusp, hence; the second-order phase transition temperature occurs at $T_C = 0.150$ ($\lambda_{qn'}$ and $\lambda_{qn''}$ correspond to the $F_{1/2}$ and FQ phases, respectively); then both $\lambda_{qn''}$ and λ_{qn} make a jump discontinuity, hence we have the first-order phase transition at $T_{tQ} = 0.515$ (λ_{qn}corresponds to the $F_{3/2}$ phase); and finally, λ_{qn} and λ_{qs} make a jump discontinuity again, hence the first-order

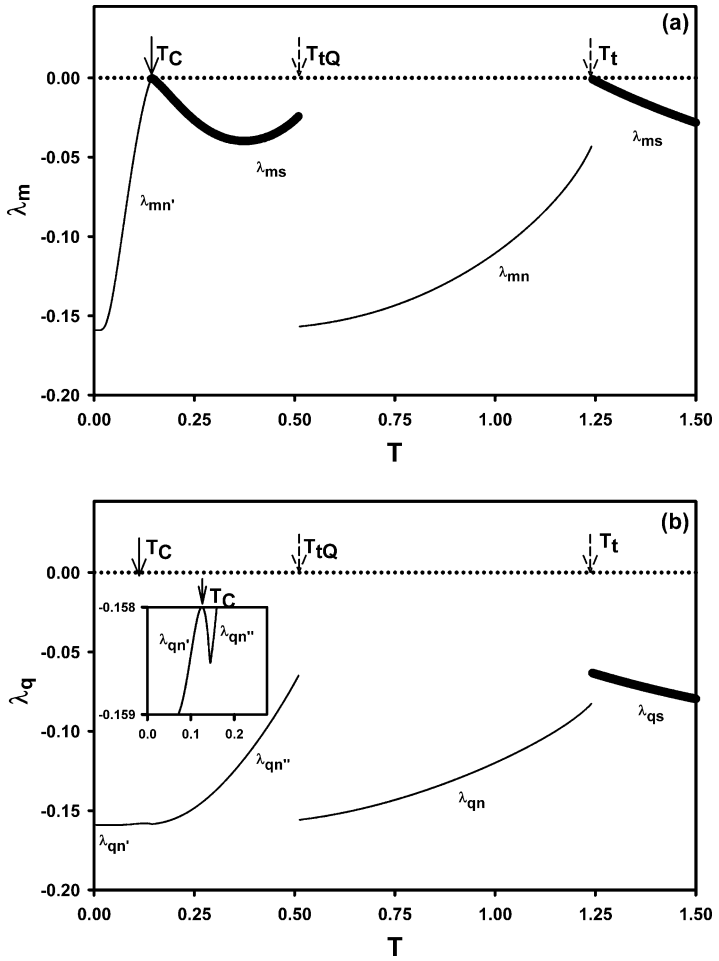

Fig. 3. The values of the Liapunov exponents as a function of the reduced temperature (T) for $k = 0.75$ and $h = 0.35$. The thick and thin lines represent the λ_s and λ_n, $\lambda_{n'}$, respectively, and T_C are the critical or the second-order phase transition for both M and Q, respectively and T_tQ is the first-order phase transition temperatures for only Q. (a) The behavior of the Liapunov exponents as a function of T for m. The system undergoes three successive phase transitions: The first one is a second-order, because $\lambda_{mn'} = \lambda_{ms} = 0$ at $T_C = 0.150$ ($\lambda_{mn'}$ corresponds to the $F_{1/2}$ phase), the second one is a first-order, because of λ_{ms} and λ_{mn} make a jump discontinuity at $T_tQ = 0.515$ (λ_{mn} corresponds to the $F_{3/2}$ phase), and the third one is also a first-order phase transition, because of λ_{mn} and λ_{ms} make a jump discontinuity at $T_t = 1.245$. (b) Same as (a), but for q. First $\lambda_{qn'}$ and $\lambda_{qn''}$ make a cusp, see the inset figure; hence the second-order phase transition temperature occurs at $T_C = 0.150$ ($\lambda_{qn'}$ and $\lambda_{qn''}$ corresponds to the $F_{1/2}$ and FQ phases); then two first-order transitions occur at $T_tQ = 0.515$ and $T_t = 1.245$, because both $\lambda_{qn''}$, λ_{qn} (λ_{qn} corresponds to the $F_{3/2}$ phase), and λ_{qn}, λ_{qs} make a jump discontinuity.

phase transition temperature occurs at $T_t = 1.245$. If one compares Fig. 3 with Fig. 2(e), one can see that T_C, T_{tQ} and T_t found by using the both calculations are exactly the same. Moreover, we have also verified the stability of the solution by this calculation, because we have always found that $\lambda_m < 0$ and $\lambda_q < 0$.

Finally, it is worthwhile to mention that the oscillating external magnetic field induces the DPT points, because if one has done the calculations for the reduced external static magnetic field amplitude h, one can see that the system does not undergo any phase transitions. This fact was illustrated in the recent work,[10] seen Fig. 6 of Ref. 10.

4. PHASE DIAGRAMS

Since we have obtained and verified the DPT points in Sec. 3, we can now present the phase diagrams of the system. The calculated phase diagrams in the (T, h) plane are presented in Fig. 4 for various values of k. In these phase diagrams, the solid and dashed lines represent the second- and first-order phase transition lines, respectively and the dynamic tricritical point is denoted by a filled circle. As seen from the figure, the following nine main topological different types of phase diagrams are found.

(i) For $0 < k \leq 0.190$, Fig. 4(a) represents the phase diagram in the (T, h) plane for $k = 0.10$. In this phase diagram, at high reduced temperature (T) and reduced external magnetic field (h), the solutions are disordered (D) and at low values of T and h, they are ferromagnetic $-3/2$ ($F_{3/2}$). The boundary between these regions, $F_{3/2} \rightarrow D$, is the second-order phase line. At low reduced temperatures, there is a range of values of h in which the D and the $F_{3/2}$ phases or regions coexist, called the coexistence region, $F_{3/2} + D$. The $F_{3/2} + D$ region is separated from the $F_{3/2}$ and the D phases by the first-order phase line. The system also exhibits only one dynamic tricritical point where both first-order phase transition lines merge and which signals the change from the first- to the second-order phase transitions. Finally, we should also mention that very similar phase diagrams were also obtained in the kinetic spin-1/2 Ising model,[8] in the kinetic spin-1 BC model,[10] the kinetics of the mixed spin-1/2 and spin-1 Ising ferrimagnetic system[9] in the kinetic spin-3/2 BC model[5] and as well as in the kinetic spin-3/2 BEG model.[7] The reason why the phase diagram is similar to the one obtained for the kinetic spin-1/2 Ising and spin-1 BC models is due to the competition between J, K and h. If $0 < k \leq 0.190$, the Hamiltonian of spin-3/2 model gives similar results to the Hamiltonian of spin-1/2 Ising and spin-1 BC models. This can explicitly be seen from the ground state phase diagrams of these three models.

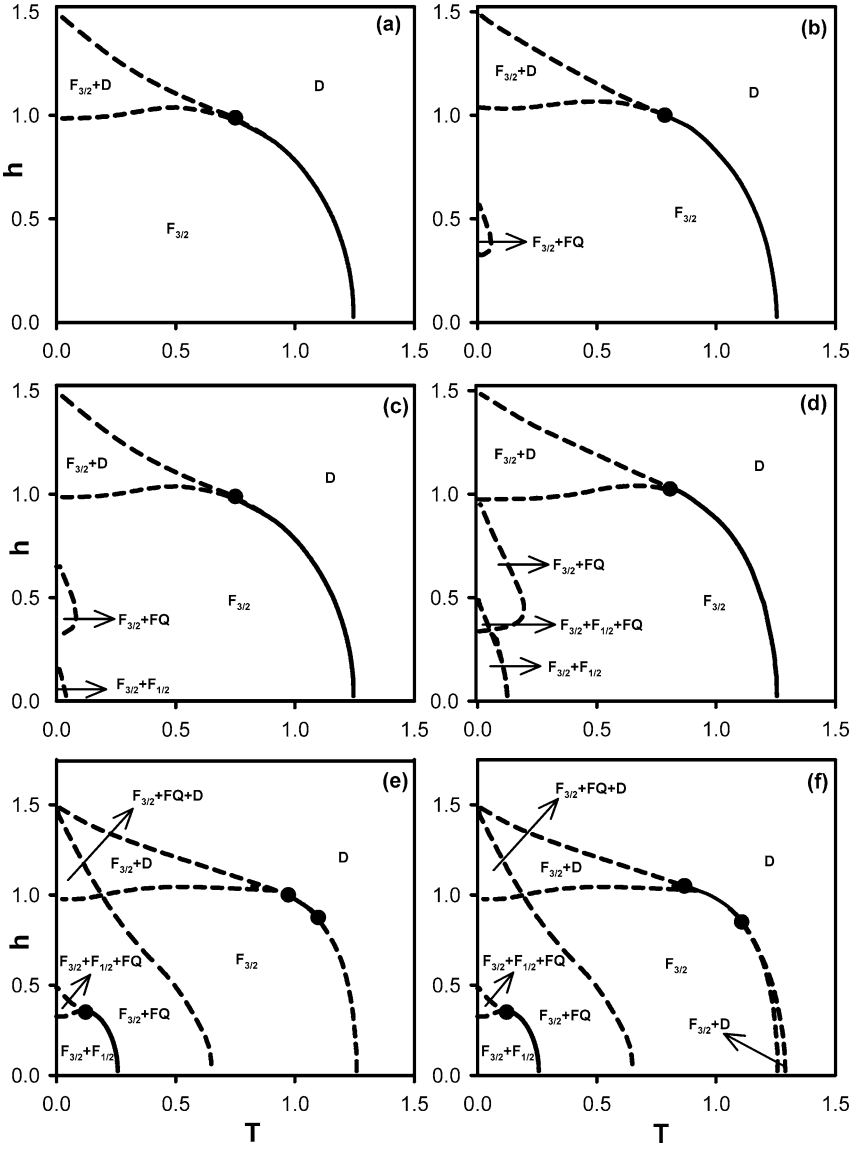

Fig. 4. Phase diagrams of the spin-3/2 Ising model Hamiltonian with arbitrary bilinear and biquadratic pair interactions in the (T, h) plane. The disordered (D), ferromagnetic-3/2 ($F_{3/2}$), and six different the coexistence regions, namely the $F_{3/2} + F_{1/2}$, $F_{3/2} + FQ$, $F_{3/2} + D$, $F_{3/2} + F_{1/2} + FQ$, $F_{3/2} + FQ + D$ and $FQ + D$ regions, are found. Dashed and solid lines represent the first- and second-order phase transitions, respectively, and the dynamic tricritical points are indicated with filled circles. (a) $k = 0.10$, (b) $k = 0.30$, (c) $k = 0.35$, (d) $k = 0.50$, (e) $k = 0.70$, (f) $k = 0.75$, (g) $k = 1.0$, (h) $k = 2.0$ and (i) $k = 4.0$.

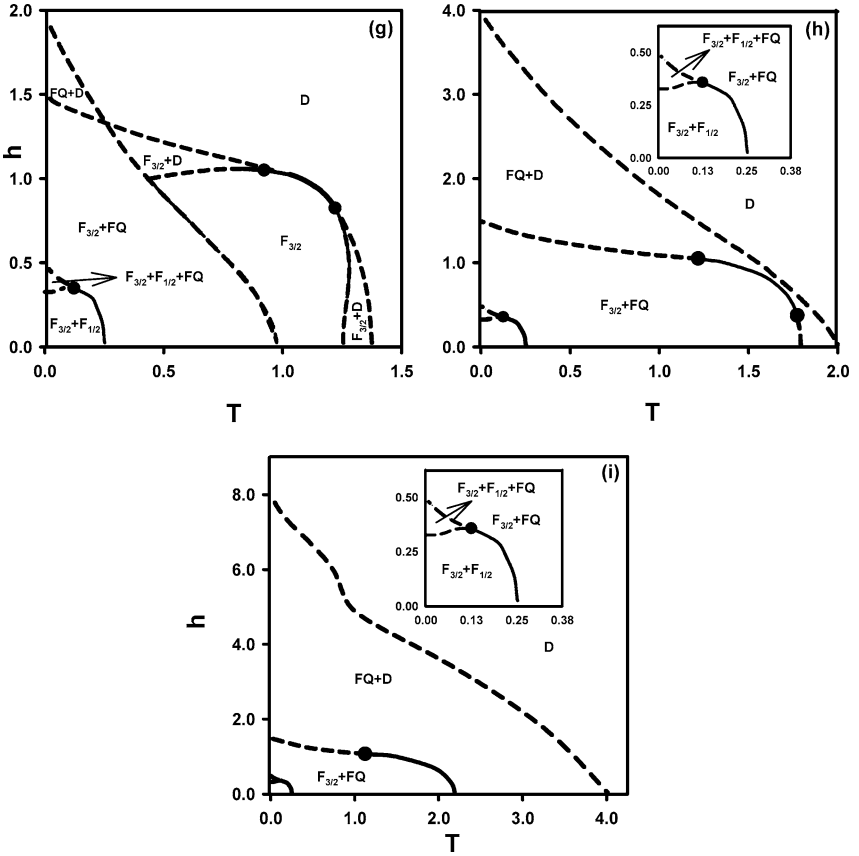

Fig. 4. Continued

(ii) For $0.190 < k \leq 0.319$, we performed the phase diagram at $k = 0.30$, seen in Fig. 4(b). This phase diagram is similar to Fig. 4(a) but only differs from Fig. 4(a) in which low values of T, and the certain range values of h, the $F_{3/2} + FQ$ phase or coexistence region also exist. The dynamic phase boundary between this $F_{3/2} + FQ$ region and the $F_{3/2}$ phase is the first-order line. Very similar phase diagram has also been found in the kinetic spin-3/2 BEG model.[7]

(iii) For $0.319 < k \leq 0.470$, we performed the phase diagram for $k = 0.35$, seen in Fig. 4(c), and is similar to the case (ii), except that the $F_{3/2} + F_{1/2}$ phase occurs for very low values of T and h. The dynamic phase boundary between the $F_{3/2} + F_{1/2}$ phase and the $F_{3/2}$ phase is also the first-order line. The similar phase diagram has also found in the kinetic spin-3/2 BEG model.[7]

(iv) For $0.470 < k \leq 0.610$, in this type the phase diagram is presented for $k = 0.50$, seen in Fig. 4(d). While this phase diagram has the same phase topology as the diagram in Fig. 4(c), but only differs from Fig. 4(c) in which the $F_{3/2} + F_{1/2}$ and $F_{3/2} + FQ$ phases or coexistence regions become large and the certain range of h they overlap each other, hence one more coexistence region, namely the $F_{3/2} + F_{1/2} + FQ$ phase also exists. The dynamic phase boundaries among these coexistence regions are all first-order line. The similar phase diagram has also been found in the kinetic spin-3/2 BEG model.[7]

(v) For $0.610 < k \leq 0.730$, the phase diagram is obtained for $k = 0.70$, seen in Fig. 4(e). This is the most interesting phase diagram in which the system exhibits three dynamic tricritical points and also five coexistence regions or phases, namely $F_{3/2} + F_{1/2}$, $F_{3/2} + FQ$, $F_{3/2} + F_{1/2} + FQ$, $F_{3/2} + FQ + D$ and $F_{3/2} + D$. The dynamic boundaries among these coexistence phases are first-order lines, except the boundary between the $F_{3/2} + F_{1/2}$ and the $F_{3/2} + FQ$ phases, this boundary is a second-order line. Since, the boundary between the $F_{3/2} + F_{1/2}$ and $F_{3/2} + F_{1/2} + FQ$, and also between the $F_{3/2} + F_{1/2} + FQ$ and the $F_{3/2} + FQ$ are first-order lines, the system exhibits a dynamic tricritical point for low values of T and h. Moreover, the dynamic phase boundary between the $F_{3/2}$ and the D phases is a first-order for low values of h and a second-order line for high values of h; hence we have a second dynamic tricritical point. A third dynamic tricritical point occurs in similar places as in the previous phase diagrams.

(vi) For $0.730 < k \leq 0.790$, we performed the phase diagram at $k = 0.75$, seen in Fig. 4(f). This phase diagram is similar to Fig. 4(e), except one more $F_{3/2} + D$ phase occurs for low values of h and high values of T. The dynamic phase boundaries between this $F_{3/2}$ and the $F_{3/2} + D$ phases and also between the $F_{3/2} + D$ and the D phases are first-order phase lines.

(vii) For $0.790 < k \leq 1.60$, in this type of the phase diagram is presented for $k = 1.0$, seen in Fig. 4(g) and is similar to the type (vi), except that the $F_{3/2} + FQ$ region becomes large and the $FQ + D$ phase appears at low values of T and high values of h. The similar phase diagram has also been found in the kinetic spin-3/2 BEG model.[7]

(viii) For $1.60 < k \leq 2.10$, we performed the phase diagram at $k = 2.0$, seen in Fig. 4(h). This phase diagram is similar to Fig. 4(g) except following differences: (1) The $F_{3/2}$ phase and the $F_{3/2} + D$ coexistence phase regions, which occur in two different places, disappear. (2) The $FQ + D$ phase region becomes very large; hence it also appears for high values of T and low values of h. The dynamic phase boundary between the $FQ + D$ and the D phase is the first-order phase line.

(ix) For $k > 2.10$, the phase diagram is constructed for $k = 4.0$, illustrated in Fig. 4(i), and is similar to type (viii), but only differs from case (viii)

in which the first-order line that occurs for the low values of h and high values of T and separates the $F_{3/2} + FQ$ phase from the $FQ + D$ phase disappears. Therefore, the dynamic tricritical point that exists for low values of h and high values of T also disappears and the system exhibits only two dynamic tricritical points.

Finally, we should point out that Fig. 4(e), (f), (h) and (i) are the new phase diagrams that have been obtained in this model.

5. SUMMARY

We have analyzed within a mean-field approach the stationary states of the kinetic spin-3/2 Ising model Hamiltonian with arbitrary bilinear and biquadratic pair interactions in the presence of a time-dependent oscillating external magnetic field. We employ the Glauber transition rates to construct the mean-field dynamical equations. We have studied the behavior of the time-dependence order parameters, namely magnetization or the dipole moment and the quadruple moment in a period, also called the dynamic magnetization and dynamic quadruple moment, as a function of reduced temperature. The DPT points are found by investigating the behavior of the dynamic order parameters as a function of the reduced temperature. Finally, we present the phase diagrams in the (T, h) plane. We found that the behavior of the system strongly depends on the values of k and nine different phase diagram topologies are found. The phase diagrams exhibit the D, $F_{3/2}$ and/or the $F_{3/2} + F_{1/2}$, $F_{3/2} + D$, $F_{3/2} + FQ$, $F_{3/2} + F_{1/2} + FQ$, $F_{3/2} + FQ + D$ and/or $FQ + D$ coexistence regions depending on k values and the dynamic phase boundaries among these phases and coexistence phase regions are mostly first-order lines, except the boundary between the $F_{3/2}$ and D phases and this boundary mostly is a second-order, seen in Fig. 4. Moreover, the dynamic phase boundaries between the $F_{3/2} + F_{1/2}$ and $F_{3/2} + FQ$ phases are mostly second-order lines. Therefore, one, two or three dynamic tricritical points also occur. We have also calculated the Liapunov exponents to verify the stability of solutions and the DPT points.

We should also mention that although similar phase diagram of Fig. 4(a) has been obtained for kinetic spin-1/2 Ising model,[8] the kinetics of a mixed Ising ferrimagnetic system,[9] the kinetic spin-1 BC model,[10] kinetic spin-3/2 BC[5] and spin-3/2 BEG models,[7] and a similar phase diagram of Fig. 4(b)–(d) and (g) have been only found in kinetic spin-3/2 BEG model;[7] the phase diagrams of Fig. 4(e), (f), (h) and (i), i.e. four phase diagrams, are the new type of phase diagrams in which have been only obtained in this model, namely the kinetic spin-3/2 Ising model Hamiltonian with arbitrary bilinear and biquadratic pair interactions in the presence of a time dependent oscillating magnetic field by using the Glauber-type stochastic dynamics.

Finally, it is worthwhile to mention that there is a strong possibility that at least some of the first- order transitions and multicritical points seen in the mean-field results are very likely artifacts of the approximation. This is because, for field amplitude less than the coercive field (at the temperature less than the static ferro-para (or order-disorder) transition temperature), the response magnetization and as well as the quadrupolar moment vary periodically but asymmetrically even in the zero-frequency limit; the system may remain locked to one well of the free energy and can not go to the other well, in the absence of noise or fluctuations [27(a), 28(d), 29, 31(a and c), 42]. However, this mean-field dynamic study suggests that the spin-3/2 Ising model Hamiltonian with arbitrary bilinear and biquadratic pair interactions in the presence of a time dependent oscillating external magnetic field has an interesting dynamic behavior, quite different from the standard Ising model. Therefore, it would be worthwhile to further study it with more accurate techniques such as dynamic Monte Carlo simulations or renormalization group calculations.

ACKNOWLEDGMENTS

This work was supported by the Technical Research Council of Turkey (TÜBITAK) Grant No. 105T114 and Erciyes University Research Funds, Grant No. FBA-06-01. We are very grateful to Bayram Deviren and Ersin Kantar for useful discussions.

REFERENCES

1. J. Sivardiére and M. Blume, Dipolar and quadrupolar ordering in spin-3/2 Ising systems. *Phys. Rev. B* **5**:1126 (1972).
2. M. Keskin and O. Canko, Theory of relaxation phenomena in a spin-3/2 Ising system near the second-order phase transition temperature. *Phys. Lett. A* **348**:9 (2005).
3. O. Canko and M. Keskin, Spin-3/2 Ising model by the Cluster variation method and the path probability method. *Physica. A* **363**:315 (2006).
4. B. C. S. Grandi and W. Figueiredo, Short-time dynamics for the spin-3/2 Blume-Capel model. *Phys. Rev. E* **70**:056109 (2004).
5. M. Keskin, O. Canko and B. Deviren, Dynamic phase transition in the kinetic spin-3/2 Blume-Capel model under a time-dependent oscillating external. *Phys. Rev. E* **74**:011110 (2006).
6. R. J. Glauber, Time-dependent statistics of the Ising model. *J. Math. Phys*. **4**:294 (1963).
7. O. Canko, B. Deviren and M. Keskin, Dynamic phase transition in the spin-3/2 Blume- Emery-Griffith model in an oscillating field. *J. Phys.: Condens. Matter.* **18**:6635 (2006). In this paper, the $F_{3/2} + FQ$ coexistence region which occurs for high values of T and low values of h should be the $F_{3/2} + D$ phase in Fig. 6(e) and (f).
8. T. Tomé and M. Oliveira, Dynamic phase transition in the kinetic Ising model under a time-dependent oscillating field. *J Phys. Rev. A* **41**:4251 (1990).
9. G. M. Buendía and E. Machado, Kinetics of a mixed Ising ferrimagnetic system. *Phys. Rev. E* **58**:1260 (1998).

10. M. Keskin, O. Canko and Ü. Temizer, Dynamic phase transition in the kinetic spin-1 Blume-Capel model under a time-dependent oscillating external field. *Phys. Rev. E* **72**:036125 (2005).
11. M. Keskin, O. Canko and E. Kantar, Dynamic dipole and quadrupole phase transitions in the kinetic spin-1 model. *Physica A* submitted.
12. P. M. Levy, P. Morin, and D. Schmitt, Large quadrupolar interactions in rare-earth compounds. *Phys. Rev. Lett*. **42**:1417 (1979); J. Kötzler and G. Raffius, Effect of quadrupolar interactions on the magnetic transitions of the terbium-monopnictides. *Z. Phys. B* **38**:139 (1980).
13. R. Aléonard and P. Morin, TmCd quadrupolar ordering and magnetic interactions. *Phys. Rev. B* **19**:3868 (1979).
14. P. Morin, J. Rouchy and D. Schmitt, Cooperative Jahn-Teller effect in TmZn. *Phys. Rev. B* **17**:3684 (1978).
15. P. M. Levy, A theoretical study of the elastic properties of dysprosium antimonide. *J. Phys. C* **6**:3545 (1973).
16. J. Kötzler, G. Raffius, A. Loidl and C. M. E. Zeyen, Singlet-Groundstate magnetism in TbP: I. static magnetic properties. *Z. Phys. B* **35**:125 (1979).
17. C. Jaussaud, P. Morin and D. Schmitt, Quadrupolar interactions in TmCu. *J. Magn. Magn. Mat.* **22**:98 (1980).
18. A. Loidl, K. Knorr, M. Müllner and K. H. J. Buschow, Magnetic properties of some rare earth magnesium compounds ($PrMg_2$). *J. Appl. Phys*. **52**:1433 (1981).
19. H. H. Chen and P. M. Levy, Dipole and quadrupole phase transitions in spin-1 models. *Phys. Rev. B* **7**:4267 (1973); M. Tanaka and I.Mannari, Phase transitions of a solvable spin-one system with bilinear and biquadratic interactions. *J. Phys. Soc. Jpn.* **41**:3 (1976).
20. K. G. Chakraborty, Effective-field model for a spin-1 Ising system with dipolar and quadrupoar interactions. *Phys. Rev. B* **29**:3 (1984); J. W. Tucker, The effective-field theory of the isotropic Blume-Emery-Griffths model. *J. Phys. C: Sol. State Phys.* **21**:6215 (1988); K. G. Chakraborty, The re-entrant behaviour of the spin-1 Ising model in the effective-field approximation. *J. Phys. C: Sol. State. Phys.* **21**:2911 (1988); A. F. Siqueira and I. P. Fittipaldi, Critical temperature for a spin Ising model with dipolar and quadrupolar interactions. *Phys. Rev. B* **31**:9 (1985); K. G. T. Chakraborty and T. Morita, A spin-one Ising model on the Bethe lattice. *Physica A* **129**:415 (1985).
21. M. Keskin, M. Arı and P. H. E. Meijer, Stable, metastable and unstable solutions of a spin-1 Ising system obtained by the molecular-field approximation and the path probability method. *Physica A* **157**:1000 (1989). M. Keskin and P. H. E. Meijer, Dynamics of a spin-1 model with the Pair correlation. *J. Chem. Phys*. **85**:7324 (1986).
22. O. Özsoy and M. Keskin, Critical properties of a spin 3/2 Ising model with bilinear and biquadratic interactions. *Physica A* **319**:404 (2003); O. Canko and M. Keskin, Analytical expressions of the order parameters near the transition temperatures in the spin 3/2 Ising system with bilinear and biquadratic interactions. *Int. J. Mod. Phys. B* **20**: 4, (2006).
23. D. K. Ray and Sivardiére, Dipolar and quadrupolar orderings in the Γ_3-Γ_5 magnetic system. J. *Phys. Rev. B* **18**:1401 (1978); W. Phystasz, Dipolar and quadrupolar phase transitions in the spin $S = 2$ cubic crystal-field system. *Phys. Rev. B* **37**:9813 (1988); M. Dudzinski, G. Faith and J. Sznajd, Magnetic and quadrupolar order in a one-dimensional ferromagnet with cubic crystal-field anisotropy. *Phys. Rev. B* **59**:13764 (1999).
24. P. Morin and D. Schmitt, Magnetic and quadrupolar phase transitions in cubic rare-earth intermetallic compounds. *Phys. Rev. B* **27**:4412 (1983).
25. K. Harada and N. Kawashima, Quadrupolar order in isotropic Heisenberg models with biquadratic interaction. *Phys. Rev. B* **65**:052403 (2002).
26. J. F. F. Mendes and E. J. S. Lage, Dynamics of the infinite ranged Potts model. *J. Stat. Phys*. **64**:653 (1991).

27. M. Acharyya, Nonequilibrium phase transition in the kinetic Ising model: Critical slowing down and the specific-heat singularity. *Phys. Rev. E* **56**:2407 (1997); A. Chatterjee and B. K. Chakrabarti, Fluctuation cumulant behavior for the field-pulse-induced magnetization-reversal transition in Ising models. *Phys. Rev. E* **67**:046113 (2003).
28. S. W. Sides, P. A. Rikvold and M. A. Novotny, Kinetic Ising model in an oscillating field: Finite-size scaling at the dynamic phase transition. *Phys. Rev. Lett*. **81**:834 (1998); S. W. Sides, P. A. Rikvold and M. A. Novotny, Kinetic Ising model in an oscillating field: Avrami theory for the hysteretic response and finite-size scaling for the dynamic phase transition. *Phys. Rev. E* **59**:2710 (1999); G. Korniss, C. J. White, P. A. Rikvold and M. A. Novotny, Dynamic phase transition, universality, and finite-size scaling in the two-dimensional kinetic Ising model in an oscillating field. *Phys. Rev. E* **63**:016120 (2001); G. Korniss, P. A. Rikvold and M. A. Novotny, Absence of first-order transition and tricritical point in the dynamic phase diagram of a spatially extended bistable system in an oscillating field. *Phys. Rev. E* **66**:056127 (2002).
29. B. K. Chakrabarti and M. Acharyya, Dynamic transitions and hysteresis. *Rev. Mod. Phys*. **71**:847 (1999).
30. A. Krawiecki, Dynamical phase transition in the Ising model on a scale-free network. *Int. J. Mod. Phys. B* **19**:4769 (2005).
31. M. F. Zimmer, Ising model in an oscillating magnetic field: Mean-field theory. *Phys. Rev. E* **47**:3950 (1993); M. Acharyya and B. K. Chakrabarti, Response of Ising systems to oscillating and pulsed fields: Hysteresis, ac, and pulse susceptibility. *Phys. Rev. B* **52**:6550 (1995); M. Acharyya, Nonequilibrium phase transition in the kinetic Ising model: Is the transition point the maximum lossy point? *Phys? Rev. E* **58**:179 (1998); H. Fujisaka, H. Tutu and P. A. Rikvold, Dynamic phase transition in a time-dependent Ginzburg-Landau model in an oscillating field. *Phys. Rev. E* **63**:036109 (2001).
32. H. Tutu and N. Fujiwara, Landau theory of dynamic phase transitions and systematic perturbation expansion method for getting phase diagrams. *J. Phys. Soc. Jpn*. **73**:2680 (2004).
33. M. Khorrami and A. Aghamohammadi, Dynamical phase transition of a one-dimensional kinetic Ising model with boundaries. *Phys. Rev. E* **65**:056129 (2002).
34. Q. Jiang, H. N. Yang and G. C. Wang, Scaling and dynamics of low-frequency hysteresis loops in ultrathin Co films on a Cu(001) surface. *Phys. Rev. B* **52**:14911 (1995); Q. Jiang, H. N. Yang and G. C. Wang, Field dependent resonance frequency of hysteresis loops in a few monolayer thick Co/Cu(001) films. *J. Appl. Phys*. **79**:5122 (1996).
35. W. Kleemann, T. Braun, J. Dec and O. Petracic, Dynamic phase transitions in ferroic systems with pinned domain walls. *Phase Trans.* **78**:811 (2005).
36. H. Jang and M. J. Grimson, Hysteresis and the dynamic phase transition in thin ferromagnetic films. *Phys. Rev. E* **63**:066119 (2001); H. Jang, M. J. Grimson and C. K. Hall, Dynamic phase transitions in thin ferromagnetic films. *Phys. Rev. B* **67**:094411 (2003); H. Jang, M. J. Grimson, and C. K. Hall, Exchange anisotropy and the dynamic phase transition in thin ferromagnetic Heisenberg films. *Phys. Rev. E* **68**:046115 (2003).
37. T. Yasui, H. Tutu, M. Yamamoto and H. Fujisaka, Dynamic phase transitions in the anisotropic *XY* spin system in an oscillating magnetic field. *Phys. Rev. E* **66**:036123 (2002); **67**:019901 (E) Erratum: Dynamic phase transitions in the anisotropic *XY* spin system in an oscillating magnetic field (2003).
38. E. Machado, G. M. Buendia, P. A. Rikvold and R. M. Ziff, Response of a catalytic reaction to periodic variation of the CO pressure: Increased CO_2 production and dynamic phase transition. *Phys. Rev. E* **71**:016120 (2005).
39. M. Acharya, Nonequilibrium phase transitions in model ferromagnets. *Int. J. Mod. Phys. C* **16**:1631 (2005).
40. See, e.g., J. C. Xavier, F. C. Alcaraz, D. Lara. Penã and J. A. Plascak, Critical behavior of the spin-3/2 Blume-Capel model in two dimensions. *Phys. Rev. B* **57**:11575 (1998); A. Bakchich and

M. El Bouziani, Position-space renormalization-group investigation of the spin-3/2 Blume-Emery-Griffiths model with repulsive biquadratic coupling. *J. Phys.: Condens. Matter.* **13**:91 (2001).
41. See. e.g., L. Peliti and M. Saber, The spin-3/2 Blume-Capel model on a honeycomb lattice. *Phys. Stat. Sol. (b)* **195**:537 (1996); J. W. Tucker, Cluster variational theory of spin-3/2 Ising models. *J. Magn. Magn. Mat*. **214**:121 (2000).
42. M. Acharyya, Nonequilibrium phase transitions in the kinetic Ising model: Existence of a tricritical point and stochastic resonance. *Phys. Rev. E* **59**:218 (1999).